Survey of the Central Plug Shape of the Aerospike Nozzle

A. Shahrokhi[1], S. Noori[2]

[1] Faculty Member, [2] Senior Researcher
Aerospace Research Institute, Ministry of Science Research and Technology,
P.O. Box 14665-834, Tehran, Iran
Tel: +98-21-8362010, Fax: +98-21-8362011
E-mail: Shahrokhi@aut.ac.ir

Abstract

To study the influence of the plug shape of an aerospike nozzle, a number of axisymmetric plugs are generated in the current research. Plug shapes are produced using uniform Cubic B-Spline curve. B-Spline method defines arbitrary shapes using a number of control points around the geometry. The flow field is simulated using Navier-Stokes equations and k-ε turbulence model. A triangle unstructured grid is applied for discretization of the governing equations. The computational methodology utilizes steady state density-based formulation. A finite volume cell centered scheme is used to discretize the flow field equations. To accelerate the solution convergence, the flow field is divided into several zones with appropriate initial conditions for each zone. The flow field around the aerospike nozzle is computationally resolved implementing various spike shapes and the best configuration is determined considering the total thrust force as a performance parameter.

Nomenclature

C_P	specific heat at constant pressure (J/kgK)
F	thrust (N)
h	altitude (m)
I_{sp}	specific impulse (s)
L	length (m)
$\dot{m}$	mass flow rate (kg/s)
M	Mach number
P	absolute static pressure (N/m^2)
T	absolute static temperature (K)
r	radial coordinate
x	axial coordinate
γ	ratio of specific heats, C_p/C_v

Subscripts

l	stagnation
e	exhaust
i	inlet
t	throat

Introduction

The aerospike rocket engine consists of a rocket thruster cowl, an aerospike nozzle, and a plug base region (Figure 1). The flow-field structure changes dramatically from low to high altitude on the spike surface and in the base-flow region [8], [7]. The aerospike adjusts to the ambient pressure and integrates well with launch vehicles which face a wide variety of altitudes during the flight [13]. In some cases a truncated spike or plug nozzle is used that provides flow injection in the base region to create an aerodynamic spike [5]. The injected flow increases the base pressure, thus the contribution of the base region to the aerospike thrust.
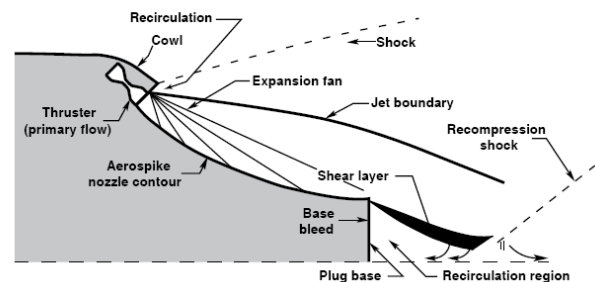

Figure 1. Aerospike components and flow field characteristics

In theory, the optimal thrust for a given jet or rocket engine occurs when the nozzle exit pressure equals the surrounding pressure. At altitudes lower than the design altitude, the thrust force is decreased as a result of over-expansion of the exhaust flow. Beside the inherent loss of thrust, the conventional nozzle might suffer problems like shock waves and flow separation in the divergent section, thrust oscillation, and flow asymmetry in over-expansion conditions. Compared to the conventional bell nozzles, unbounded expansion of the jet provides overly better performance in Aerospike nozzles. Besnard and his group applied the axisymmetric aerospike nozzle in propulsion system of sounding rockets and demonstrated considerable gain in the performance of the rockets [3].

In the aerospace literature it has been documented that the flow in supersonic nozzle is substantially influenced by viscous effects which reduce the performance of the propulsion system [7], [8]. In many cases, the Reynolds number of the flow over the plug is high enough to oblige a turbulence flow along the nozzle spike. Koutsavdis applied several turbulence models for the computation of a plug nozzle flow field and compared the results with experimental observations [9].

One of the key points about the aerospike nozzle is the selection of a suitable shape that can provide the maximum thrust force.

One of the most popular methods for curve representation which is used in this research is B-Spline. This method introduces control points around the geometry. These points are then used to define the arbitrary shape. Several researchers employed B-spline approach to parameterize the aerodynamic shapes during the optimization process [2],[12]. This method for defining the shape possesses acceptable flexibility in generating spikes with different curvature and inclinations while offering smooth curves. To generate the spike configurations, cubic B-Spline method is used and the flow field is resolved for each case. The best shape is selected comparing the relevant thrust force of different shapes.

Geometry of the Plug Nozzle

Approximate methods have been used to design the initial central plug of the aerospike nozzle [3]. B-Spline method is able to define different plug nozzle configurations. These plugs are generated using a number of control points around the geometry [1]. x and y coordinates of the surfaces are written in a parametric form.

$$x(u) = \sum_{i=1}^{n+1} X_i N_{i,k}(u)$$

$$(n \geq k-1)$$

$$y(u) = \sum_{i=1}^{n+1} Y_i N_{i,k}(u) \qquad (1)$$

x and y are the Cartesian coordinates of the surface, $N_{i,k}$ is the i*th* B-spline basis function of order k. u is the parameter variable and (X_i, Y_i) are the coordinates of the B-Spline control points. Therefore B-Spline basis functions of an arbitrary dimension *n* can be evaluated as linear combinations of basis functions of a degree lower. B-Spline basis functions are obtained using De boor's relation.

$$N_{i,k}(u) = \frac{u - u_i}{u_{i+k-1} - u_i} N_{i,k-1}(u) \qquad (2)$$

$$+ \frac{u_{i+k} - u}{u_{i+k} - u_{i+1}} N_{i+1,k-1}(u)$$

Where $N_{i,1}(u) = \begin{cases} 1, & u_i < u < u_{i+1} \\ 0, & otherwise \end{cases} \qquad (3)$

u_i is the non-decreasing set of real numbers called knot sequence. The number of knots is equal to the dimension of the basis function plus the order of the B-Spline curve. Since the basis functions are based on knot differences, the shape of the basis function is only dependent on the knot spacing and not specific knot values. Comparing with other polynomials, B-Spline curves have the advantage of limiting the dimension of the polynomial to a user-defined level without changing the number of control points.
B-Spline of order 3 is used in this research together with 16 control points. The first and the last control points are fixed. Seven different shapes are generated which are shown in figure 2.

Numerical Simulations and Analysis

Details of numerical simulation and analysis of internal and external flow of aerospike nozzles have been extensively described in [11]. However, some aspects of numerical modelling which are specifically important in analysis of aerospike nozzles with base bleed are highlighted herein. The numerical analysis of internal and external flow of the aerospike nozzle is performed using Navier-Stokes equations considering turbulent flow. The computational methodology utilizes steady state density-based formulation and a finite volume cell centered scheme to discretize the flow field equations.
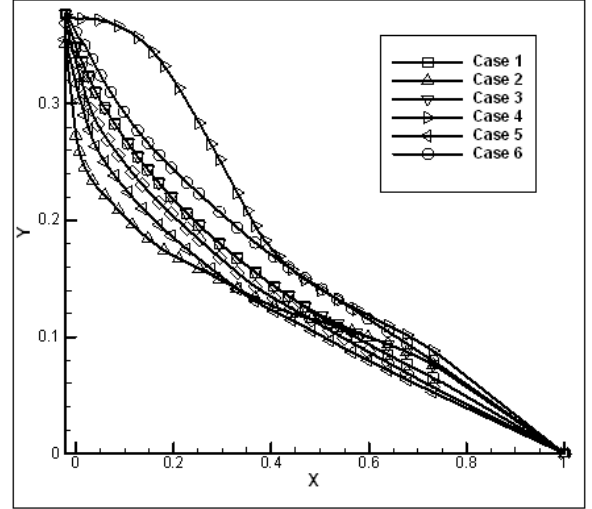

Figure 2. Spike shapes generated using Cubic B-Spline

The viscous terms are evaluated using central difference and the standard k-ε scheme is utilized to simulate the eddy viscosity. The flow is assumed to be axisymmetric although three-dimensional equations are used for this study. The flow field is divided into several zones. Each zone is facilitated with proper unstructured triangle grid and the appropriate initial conditions. Providing the control over the grid density and initial conditions in different zones is helpful in accelerating the solution convergence. The grid density increases towards the throat and the remaining computational domain coarseness increases outward the nozzle outlet.

Average properties of combustion products resulting from chemical reaction of ethanol and oxygen have been assumed for the fluids in all regions. These properties, which satisfy the following relation:

$$C_P = \frac{\gamma \Re}{\mathcal{M}(\gamma - 1)} \qquad (4)$$

Where,
γ = 1.21
C_P = 1286.68 J/kgK
M = 37.23 g/mol.

The condition implied at the inlet of the convergent section is inlet with specified mass flow of 3.25757 kg/s, total temperature of 1577.826 K and the pressure of 2045430 N/m².
In this work, the convergence is investigated using two criteria. One of them is reduction of the global residual of solution of all governing equations to the order of 10^{-5}, and the other is establishment of mass balance among inlet, far-field and outlet boundaries, which is checked by integration of mass flow through the mentioned boundaries in each iteration. The solution process has been continued in all shapes until both criteria are satisfied.
One of the most suitable criteria for measurement the performance of an aerospike nozzle is the thrust of the propulsion system. For an axisymmetric aerospike nozzle, thrust is calculated using momentum flux integrals and the surface pressure over the throat and plug.

Results and Discussions

This section describes numerical modelling and analysis of internal and external flow of different aerospike nozzle shapes

introduced in previous sections. The objective of the analysis is the comparison of the thrust calculated employing Navier-Stokes equations with standard k-ε model.

The inlet properties of the convergent part with a length of L=0.2m considered here are:

A_i= 7.212855×10^{-3} m^2 ,A_i/A_t=5.01384
M_i = 0.13
P_i = 0.98984, P_0 = 2045430 N/m^2

Figure 3. Grid Distributions in the flowfield

The entire solution domain for the aerospike nozzle is displayed in Figure 3. To provide the solution domain with different initial conditions, it is divided into 4 regions. The grid independency is checked using three different resolutions resulting in 149644, 188517 and 191097 cells and the computed thrust force for each case is 3151.68 N, 3282.03N and 3283.86 respectively. Therefore the second case is chosen as the most appropriate resolution. Considering axial symmetry of the problem, numerical solution is carried out in half of the entire domain, bounded by a boundary with axial symmetry condition. Figure 4 shows the grid distribution in the convergent part of the nozzle and near the plug.

The numerical results are validated against the computed thrust in ref. 4 for the design conditions when $P_{atm}/P_{design} = 1.0$. The resulted thrust in this case is 4414.79 N and the optimum thrust obtained in ref. 4 is 4443.93 N. The following results are obtained for an overexpansion case with $P_{atm}/P_{design} = 4.0$.

The flow properties are computed for the aerospike nozzles considering six spike shapes introduced in figure 2. The Mach number contours are shown in figure 5 for case 1. As seen in the figure, a strong shock occurs downstream of the convergent part of the nozzle. Figure 6 illustrates Mach number contours for case 2. Comparing with case 1, the shock wave is moved downwards. The Mach number contours of case 3 are demonstrated in figure 7. According to this figure, there are two shocks over the spike but they are smaller than the shockwave occurs over the spike of the case 1.

Mach contours of case 4 are shown in figure 8. The shockwave is reduced in this case. To provide more reduction in the shockwave strength, the gradient of the leading part of the spike is decreased in case 5. Figure 9 illustrates Mach number of case 5. The figure shows the reduction in the second shockwave along the spike but the first shockwave is decreased at the beginning of the spike. Therefore the gradient of the spike is increased in case 6. Mach contours of this case are shown in figure 10. The shockwave strength is comparably reduced in this case.
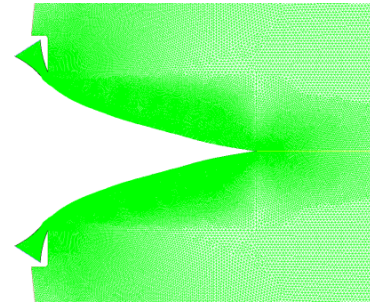

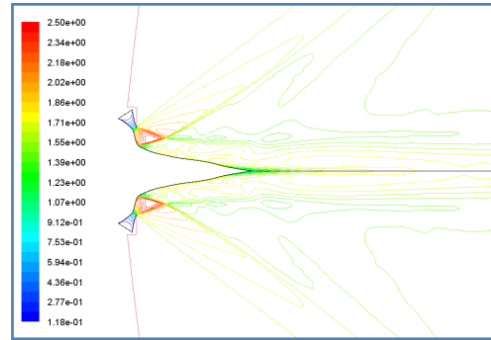Figure 4. Grid Distributions in the flow field

Figure 5. Mach number Contours, case 1
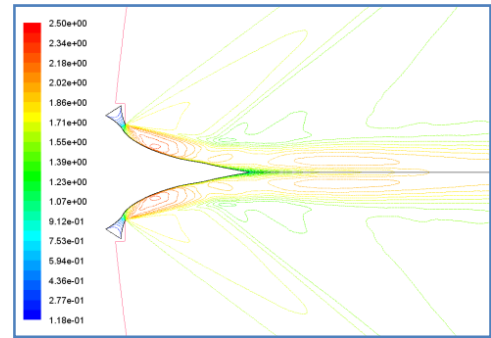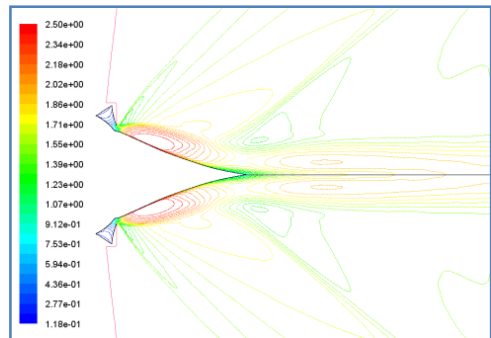

Figure 6. Mach number Contours, case 2

Figure 7. Mach number Contours, case 3

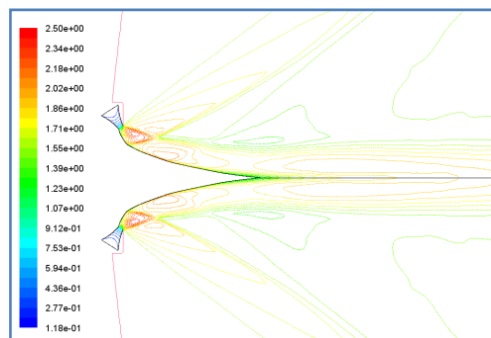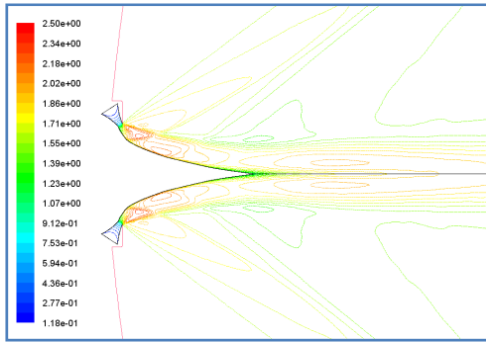Figure 8. Mach number Contours, case 4
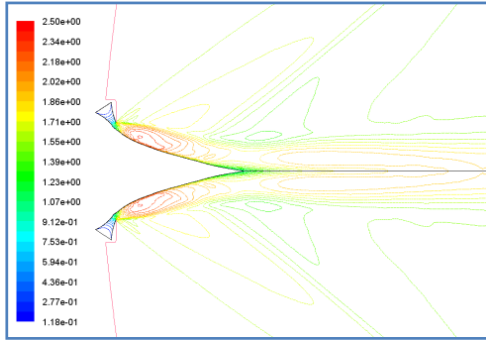
Figure 9. Mach number Contours, case 5

Figure 10. Mach number Contours, case 6

Table 1- Thrust Force for Different Spike shapes

Different plug shapes	T1	T2	T3	Total Thrust
Case 1	1017.77	767.28	1086.09	2871.14
Case 2	1004.28	795.16	1449.49	3248.93
Case 3	921.53	1021.24	1081.59	3024.36
Case 4	1018.67	761.53	1316.67	3096.87
Case 5	1015	770.84	1394.69	3180.89
Case 6	809.78	809.78	1453.27	3249.18

The thrust force of the six cases introduced previousely is calculated using equation (5). Table (1) shows the value of the thrust for each case. The three components of the thrust shown in this table are the terms of the thrust in equation (5). The last term (T_3) indicates the thrust over the spike part of the nozzle. The maximum spike thrust force and also the maximum total thrust are related to case 6. The minimum thrust is related to case 3 which has the steepest gradient.

Conclusion

In the current research the flow properties of different aerospike nozzle shapes have been studied. The flow field was simulated using Navier-Stokes equations and k-ε turbulence model. Different plug shapes were generated using uniform Cubic B-Spline curve. Total thrust force was considered as a performance parameter and the best configuration was determined.

References

[1] Anderson, K.W., Bonhaus, D.L., Airfoil Design on Unstructured Grids for Turbulent Flows, AIAA Journal, Vol. 37, No. 2, Feb. 1999, pp. 185-191.

[2] Anderson,K.W., Venkatakrishnan,V., Aerodynamic Design Optimization on Unstructured Grid with a Continuous Adjoint Formulation, AIAA Paper 97-0643, Jan 1997.

[3] Angelino G., "Approximation Method for Plug Nozzle Design", AIAA Journal, Vol. 2, No. 10, Oct. 1964, pp. 1834-1835.

[4] Besnard, E., H. H. Chen, T. Mueller and J. Garvey, "Design, Manufacturing and Test of a Plug Nozzle Rocket Engine", AIAA Paper 2002-4038, 2002.

[5] Hagemann, G., Schley, C.-A., Odintsov, E., and Sobatchkine, A., "Nozzle Flowfield Analysis with Particular Regard to 3D-Plug-Cluster Configurations," AIAA Paper 96-2954, July 1996.

[6] Iacobellis, S. F., Larson. V. R., and Burry, R. V., "Liquid-Propellant Rocket Engines: Their Status and Future," J. of Spacecraft and Rockets, Vol. 4, Dec. 1967, pp. 1569-1580.

[7] Korte J.J., Salas A. O., Dunn H.J., Asexandrov N.M., Follett W.W., Orient G.E., and Hadid A.H., Multidisciplinary Approach to Linear Aerospike Nozzle Optimization, AIAA Paper 97-3374, 1997.

[8] Korte J.J., Parametric Model of an Aerospike Rocket Engine, AIAA Paper 2000-1044, 2000.

[9] Koutsavdis, E.k., A Numerical Investigation of the Flow Characteristics of Plug Nozzle Using Fluent, 40th AIAA meeting and exhibition, Reno, NV, 2002.

[10] Mueller, T. J., and Sule, W. P., "Basic Flow Characteristics of a Linear Aerospike Nozzle Segment,"ASME Paper 72-WA/Aero-2, Nov. 1972.

[11] Noori, S. and Shahrokhi, A. "The Comparison of different Turbulence Models on the FlowField Characteristics of an Aerospike Nozzle", The ASME International Mechanical Engineering Congress & Exposition, 12-18 Nov., 2010, Vancouver, British Colombia, Canada.

[12] Obayashi, Sh., Nakahashi, K., Oyama, A., Yoshino, N., Design Optimization of Supersonic Wing Using Evolutionary Algorithms, European Congress on Computational Methods in Applied Science and Engineering (ECCOMAS) 1998.

[13] Rao, G. V. R., "Recent Developments in Rocket Nozzle Configurations," ARS Journal, Sept. 1961, pp.1488-1494.

.